Pyrrolidone-Functional Smart Polymers via Nitroxide Mediated Polymerization.

Xeniya Savelyeva[a] and Milan Marić[a,*]

[a]*McGill University, Department of Chemical Engineering, McGill Institute of Advanced Materials (MIAM), Centre for Self-Assembled Chemical Structures (CSACS),*

3610 University Street, Montréal, Québec, Canada H3A 2B2

**Corresponding author*

Email address: milan.maric@mcgill.ca (M. Marić)

Phone: (514) 398-4272, Fax: (515) 398-6678

ABSTRACT

Nitroxide mediated polymerization (NMP) of *N*-(2-methacryloyloxyethyl) pyrrolidone (MAEPYR) with 2-([*tert*-butyl[1-(diethoxyphosphoryl)-2,2-dimethylpropyl]amino]oxy)-2-methylpropanoic acid (BlocBuilder) initiator and *N*-tert-butyl-*N*-[1-diethylphosphono-(2,2-dimethylpropyl)] (SG1) nitroxide permitted controlled synthesis of poly(*N*-(2-methacryloyloxyethyl)-pyrrolidone-*stat*-9-(4-vinylbenzyl)-9H-carbazole) (poly(MAEPYR-*stat*-VBK)) statistical copolymers. With at least 5 mol% VBK, the dispersity Đ of the copolymers was below 1.4 at conversions less than 50%. At conversions higher than 50%, and at lower VBK feed content, there was a significant amount of termination reactions, which broadened the molecular weight distribution of the final polymers (Đ = 1.4 - 2.3). The MAEPYR-rich statistical copolymers were subsequently tested for thermo-responsive behaviour in aqueous media. The cloud point temperatures (CPT) in aqueous solution were tuned by changing the VBK composition, solution concentration and heating rate, and the transitions were thermally reversible with partial loss of reversibility at higher heating rates. The CPT decreased from 59.0 °C to 49.7 °C with addition of only 1 mol% of VBK in the copolymer, and at more than 6 mol% VBK, the copolymer was water-insoluble.

KEYWORDS: copolymerization, *N*-(2-methacryloyloxyethyl)-pyrrolidone (MAEPYR), BlocBuilder, nitroxide mediated polymerization (NMP), stimuli-sensitive polymers, cloud point temperature (CPT).

INTRODUCTION

A functional material that can respond to different external stimuli is a key towards developing a new generation of intelligent or "smart" materials. The response of such materials can be regarded as a change in shape, solubility, and surface characteristics[1], usually with an attendant reversibility. The stimuli for these transitions can be a change in temperature[2], pH[3], ionic strength[3], light[4] or presence of certain metabolic chemicals[5]. Materials that can undergo a phase transition in response to the changes in the metabolic variables of biological fluids, (temperature and/or pH) are of special interest[6] in a wide range of applications, such as drug delivery, biosensors, tissue engineering, coatings, textiles and optical systems. As the most widely used stimulus[7], temperature can be easily controlled and applied both *in vivo*[8, 9] and i*n vitro*[10, 11]. Many temperature sensitive polymers exhibit a lower critical solution temperature (LCST) in water, which is the critical point where a polymer becomes water-insoluble upon heating.[12] Poly(*N*-isopropylacrylamide) (PNIPAM) has become the most studied temperature-sensitive polymer, particularly since its LCST is near body temperature[13-17].

The hydrophobic and hydrophilic moieties present in the chain determine the LCST of the phase transition.[7] The phase transition can be adjusted subtly by the changes in a monomer's structure. For instance, Cai and coworkers reported a decrease in cloud point temperature (CPT) of as much as 37 °C from the acrylic-based pyrrolidone functional homopolymers (CPT ≈ 66.5 °C, poly[*N*-(3-acryloyloxypropyl) pyrrolidone]) to the methacrylic-based pyrrolidone functional homopolymers (CPT ≈ 29.5 °C, poly[*N*-(3-methylacryloyloxypropyl) pyrrolidone]).[18] Poly(2-*N*-morpholinoethyl acrylate) (PMEA)) and poly(2-*N*-morpholinoethyl methacrylate) (PMEMA)) were analysed recently by our group for their phase transition behavior. PMEA was completely water soluble in the range of temperatures studied (20-95 °C); whereas PMEMA had a CPT at about 37 °C.[19] The higher CPT of the latter polymer can be explained by the constraint of

hydrogen bonding due to rotation of the backbone methyl groups.[17] Poly(*N*-vinyl-pyrrolidone) (PVP) is another example where the subtle changes in the molecular structure affects the phase transition. PVP is soluble in aqueous solution over a wide range of temperature; however, its analogues, where the molecular structure was modified by addition of a hydrophobic spacer, were shown to have a LCST.[18, 20] Polymers with pyrrolidone functionalities are applied in biomedical research due to their water solubility[21, 22], biocompatibility[20-22], low toxicity[21], and coordination capacity[18, 20, 22]. PVP can also be used as a blood plasma substitute[21-24], food thickener[22], binding agent for drug delivery[20, 23], and inhibitor of hydrate formation[25, 26].

Polymer microstructure influences directly the polymer properties. In the case of temperature responsive polymers, the response to temperature changes is sharp for monodisperse samples, and it is less defined for polymers with broad molecular weight distributions.[18, 27-29] Various polymerization techniques, such as living ionic polymerization, have been developed to allow the synthesis of well-defined polymers with predictable molecular weight and precise microstructure. Ionic polymerization, however, requires very stringent reaction conditions since the presence of any impurity (e.g. air, moisture) will terminate the reaction. This is where controlled radical polymerization (CRP) becomes useful. It has moderate sensitivity to the impurities, like conventional radical polymerization, and it has pseudo "living" character as in ionic polymerization since termination reactions can be sufficiently suppressed for a significant portion of the polymerization. CRP techniques do not require rigorous purification conditions to obtain well-defined polymers; therefore, small amounts of impurities are tolerated.[30] Among various techniques currently used for CRP, reversible addition-fragmentation chain transfer polymerization (RAFT)[31-34], nitroxide mediated polymerization (NMP)[22, 35-37] and atom transfer radical polymerization (ATRP)[38, 39] are the most popular ones.[39]

MAEPYR monomer (Scheme 1) shares similar properties with *N*-vinylpyrrolidone (VP) due to the common pyrrolidone functionality. Hadjichristidis and co-workers have attempted to polymerize VP via NMP using 2,2,6,6-tetramethylpiperidinyl-1-oxy (TEMPO) nitroxide.[22, 23] The final polymers were obtained at low yields with high dispersity (1.7 - 2.2) mostly due to the prevalent termination reactions present at prolonged reaction times.[23] MAEPYR has been polymerized in a controlled manner previously using RAFT[18, 40] and conventional radical polymerization[41], but not by NMP. NMP does not require removal of metallic impurities, as in the case of ATRP, nor does it use sulphur-based chain transfer agents as in the case of RAFT. It is thus valuable to see if NMP's favourable characteristics can be used for a controlled synthesis of MAEPYR polymer without impeding phase transition properties in aqueous solution. However, to apply NMP via commercially available BlocBuilder (2-([*tert*-butyl[1-(diethoxyphosphoryl)-2,2-dimethylpropyl]amino]oxy)-2-methylpropanoic acid), the methacrylate must be copolymerized with a comonomer in order to decrease the average equilibrium constant to keep the polymerization controlled. Styrene and acrylonitrile are examples of the most commonly used controlling comonomers.[42, 43] Our group has found that 9-(4-vinylbenzyl)-9H-carbazole (VBK) (Scheme 1) can be used as a very effective controlling comonomer.[19, 44-48] The VBK units not only served to control the copolymerization with reduced amount of comonomer compared to styrene, but imparted fluorescent, electron-donating functionality into the copolymers and permitted tuning of the LCST due to its relative hydrophobicity.

In this study NMP with BlocBuilder (Scheme 1) was examined to yield MAEPYR-rich copolymers when using VBK as a controlling comonomer. The activity of the copolymers' chain end was assessed by reinitiating with a fresh batch of *N*,*N*-dimethylacrylamide (DMAA)

(Scheme 1). The resulting statistical and block copolymers were solubilized in aqueous solutions and their CPTs were measured. The effect of copolymer composition, solution concentration, pH and the addition of poly(DMAA) block was studied and reported.

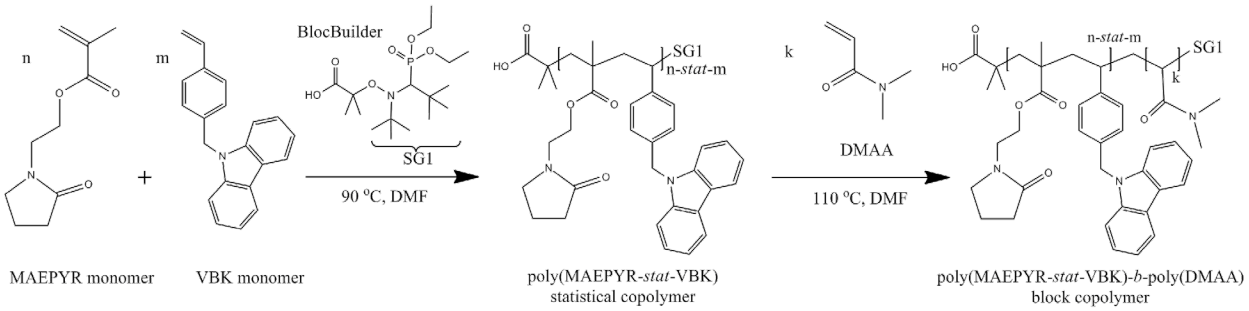

SCHEME 1 Synthetic route used to obtain poly(*N*-(2-methacryloyloxyethyl) pyrrolidone-*stat*-9-(4-vinylbenzyl)-9H-carbazole) (poly(MAEPYR-*stat*-VBK)) statistical copolymers by NMP using BlocBuilder initiator followed by the chain extension with *N*,*N*-dimethylacrylamide (DMAA) to form poly(*N*-(2-methacryloyloxyethyl) pyrrolidone-*stat*-9-(4-vinylbenzyl)-9H-carbazole)-*b*-poly(*N*,*N*-dimethylacrylamide) (poly(MAEPYR-*stat*-VBK)-*b*-poly(DMAA)) block copolymer.

EXPERIMENTAL SECTION

Materials

Calcium hydride (90-95%, reagent grade, Sigma Aldrich), basic alumina (Brockmann, type 1, 150 mesh, Sigma Aldrich), lithium bromide (ReagentPlus, ≥99%, Sigma Aldrich), 1-(2-hydroxyethyl)-2-pyrrolidone (98%, Sigma Aldrich), dimethyl sulfoxide (DMSO) (deuterated-d_6, 99%, Sigma Aldrich), methacryloyl chloride (97%, contains 200 ppm monomethyl ether hydroquinone as stabilizer, Sigma Aldrich), *N*,*N*-dimethylformamide (DMF, >95% certified ACS, and 99.5% HPLC grade, Acros Organics), ethyl ether anhydrous (>95%, BHT stabilized/certified ACS, Fisher Scientific), magnesium sulfate (anhydrous, certified powder, Fisher Scientific), sodium chloride (≥99.5, certified ACS, Fisher Scientific), sodium carbonate (anhydrous, ≥99.5, certified ACS, Fisher Scientific), and triethylamine (99 %, Fisher Scientific) were used as received. The deuterated chloroform ($CDCl_3$, >99%) was obtained from Cambridge Isotopes Laboratory and also used as received. Chloroform (>99%, reagent ACS grade, Fisher Scientific), and *N*,*N*-dimethylacrylamide (DMAA, 99%, contains 500 ppm monomethyl ether hydroquinone as stabilizer, Sigma Aldrich) were purified by passage through a column of 5 wt % calcium hydride relative to basic alumina and then stored in a sealed flask under a head of nitrogen in a fridge until needed. *N*-(2-methacryloyloxyethyl) pyrrolidone (MAEPYR) was synthesized according to the literature[40] with slight variations as noted below and stored in a sealed flask under a head of nitrogen in a refrigerator until needed. 9-(4-vinylbenzyl)-9H-carbazole (VBK) was synthesized according to the literature[49] and stored in a refrigerator away from the light source. 2-([*tert*-butyl[1-(diethoxyphosphoryl)-2,2-dimethylpropyl]amino]oxy)-2-methylpropanoic acid, also known as BlocBuilder (99%), was obtained from Arkema and used without further purification. [*tert*-butyl[1-(diethoxyphosphoryl)-2,2-

dimethylpropyl]amino]oxidanyl, also known as SG1 (>85%), was kindly donated by Noah Macy of Arkema and used as received. 2-Cyano-2-propyl dodecyl trithiocarbonate (CPDTC) was obtained from Sigma Aldrich and used without further purification. 2,2'-azobisisobutyronitrile (AIBN, Vazo 67 from Du Pont) was recrystallized from methanol.

Monomer synthesis

The esterification reaction was adopted from Cai et al.[40] with slight variations. A 125 ml 3-neck jacketed reactor, equipped with a stir bar, and a dropper column were used. Measured amounts of 1-(2-hydroxyethyl)-2-pyrrolidone (40.06 g, 0.31 mol), triethylamine (31.26 g, 0.31 mol) and anhydrous chloroform (35 ml) were added to the reactor and stirred well at 5 °C. The reaction mixture was purged with nitrogen for 20 minutes. Methacryloyl chloride (32.40 g, 0.31 mol) was diluted with anhydrous chloroform (40 ml), and then the mixture was added to the reactor drop-wise over a 1 hour period. The reaction was allowed to proceed for at least 10 hours at 10 °C. The nitrogen purge remained for the entirety of the reaction. For the purification, white ammonium salt was removed by vacuum filtration. The solution was first concentrated by rotary evaporation, and then extracted thrice using first 5 wt% Na_2CO_3 (200 ml), then saturated NaCl solution (100 ml) and deionized water (200 ml). The solution was dried under $MgSO_4$ (3 g), and concentrated by rotary evaporation to remove any solvent residuals. The monomer's structure was verified by nuclear magnetic resonance (^{1}H NMR) spectroscopy in deuterated chloroform and DMSO. The final yield was 14.7 g (24%).

^{1}H NMR (δ, in $CDCl_3$): 6.08 and 5.56 ppm (2H, CH_2=CHCH$_3$), 4.25 ppm (2H, COOCH_2CH$_2$), 3.56 ppm (2H, COOCH$_2$CH_2), 3.46 ppm (2H, NCOCH$_2$CH$_2$CH_2 in pyrrolidone ring), 2.35 ppm (2H, NCOCH_2CH$_2$CH$_2$ in pyrrolidone ring), 2.01 ppm (2H, NCOCH$_2$CH_2CH$_2$ in pyrrolidone ring), 1.91 ppm (3H, CH$_2$=CHCH_3).

Polymer synthesis

General

All the copolymerizations were performed in a 10 ml three-neck round bottom glass reactor equipped with a condenser, a temperature well with a thermocouple, and a stir bar. The reactor was placed in a heating mantle on a stir plate and a thermocouple was connected to a temperature controller. The condenser was cooled using an Isotemp 3016D (Fisher Scientific) chiller unit in order to prevent any monomer or solvent evaporation. The nitrogen purge was applied for 20 min before the reaction, and the needle was inserted into the rubber septum, used to cap the condenser, in order to vent the purge. The reactor was then heated (at 5 - 7 °C min^{-1}), and the point when the temperature reached the set point was arbitrarily chosen as t = 0 min. The purge with the reduced flow rate was kept throughout the reaction, and the samples were periodically withdrawn by syringe to track the polymerization progress. Both samples and the crude polymer were precipitated in excess of cold diethyl ether, recovered and vacuum dried at 40 °C overnight.

Synthesis of poly (N-(2-Methacryloyloxyethyl) Pyrrolidone – stat – 9-(4-Vinylbenzyl)-9H-Carbazole) (poly(MAEPYR-stat-VBK)) Statistical Copolymers via NMP.

Table 1 lists all the formulations studied. All the copolymerizations were conducted with BlocBuilder and SG1 initiators in DMF (50 wt%) at 90 °C. The molar ratio of SG1 relative to BlocBuilder (r = $[SG1]_0/[BlocBuilder]_0$) was 0.1, the VBK initial feed concentration ($f_{VBK,0}$) was varied between 2 - 10 mol%, and the target molecular weight at complete conversion was calculated to be 10, 25 or 50 kg mol^{-1}. The formulation of MV-1, with initial VBK molar composition ($f_{VBK,0}$) 2 mol%, is given as an example (Table 1). BlocBuilder (0.048 g, 0.125 mmol), SG1 (0.004 g, 0.012 mmol), MAEPYR (3.01 g, 15.28 mmol), VBK (0.085 g, 0.32

mmol), and DMF (3.10 g, 42.37 mmol) were added to the reactor. The polymerization was performed at 90 °C for 5.3 hours. Samples of 0.1 - 0.15 ml were withdrawn during the reaction to track the polymerization progress, and at the end of the reaction the final yield was 0.99 g (88% conversion; final molar composition of VBK, F_{VBK} = 0.01) with $\overline{M_n}$= 10.2 kg mol^{-1} and $\overline{M_w}/\overline{M_n}$= 1.58. The procedure for compositional analysis via NMR is shown in the characterization section. The GPC was calibrated using PMMA standards in DMF at 50 °C. The yield was determined gravimetrically and it was lower than expected. This might be due to the choice of the non-solvent used for the precipitation (diethyl ether in this case), since the low molecular weight oligomers that contributed to the overall conversion, as determined by NMR analysis, might have been washed out.

TABLE 1 Experimental formulations for poly(*N*-(2-methacryloyloxyethyl)-pyrrolidone-*stat*- 9-(4-vinylbenzyl)-9H-carbazole) (poly(MAEPYR-stat-VBK)) statistical copolymerizations performed in 50 wt% DMF solution at 90 °C.

ID[a]	Symbol	[BlocBuilder]$_0$ (mol L^{-1})	[SG1]$_0$ (mol L^{-1})	[VBK]$_0$ (mol L^{-1})	[MAEPYR]$_0$ (mol L^{-1})	[DMF]$_0$ (mol L^{-1})	$M_{n,target}$[b] (kg mol^{-1})	$f_{VBK,0}$[c]
MV-1	Δ	0.021	0.002	0.05	2.57	7.12	24.8	0.02
MV-2	○	0.051	0.005	0.10	2.45	7.38	10.0	0.04
MV-3	◊	0.020	0.002	0.10	2.47	7.34	25.2	0.04
MV-4	□	0.011	0.001	0.11	2.55	7.17	49.3	0.04
MV-5	+	0.021	0.002	0.13	2.41	7.48	24.9	0.05
MV-6	*	0.020	0.002	0.20	2.36	7.60	25.8	0.08
MV-7	x	0.020	0.002	0.25	2.21	7.94	24.9	0.10

[a] Experiments for poly(MAEPYR-stat-VBK) copolymerizations are denoted MV-Z with M representing *N*-(2-methacryloyloxyethyl)-pyrrolidone, V representing 9-(4-vinylbenzyl)-9H-carbazole, and Z representing the experiment number; [b] The target molecular weight, $M_{n,target}$, was calculated according to $M_{n,target} = M_I + M_m*[m]_0/[I]_0$, where M_I and M_m are the molecular weight of the initiator and monomer, respectively, $[m]_0$ and $[I]_0$ are the initial monomer and initiator concentrations, respectively; [c] $f_{VBK,0}$ is the initial molar fraction of VBK in the feed.

Synthesis of poly (N-(2-Methacryloyloxyethyl) Pyrrolidone – stat – 9-(4-Vinylbenzyl)-9H-Carbazole)-block-poly(N,N-Dimethylacrylamide) (poly(MAEPYR-stat-VBK)-b-poly(DMAA)) Block Copolymers via NMP.

Table 2 lists the formulations studied. The general procedure for chain extension experiments was the same as for the copolymerizations. The macroinitiator was synthesized prior to the chain extension experiment, and a fresh batch of DMAA monomer was used. A formulation for chain extension of MV-3 at 110 °C is given as an example below. Macroinitiator MV-3 (0.55 g, 0.04 mmol), DMAA (2.0 g, 20.4 mmol), and DMF (1.9 g, 25.9 mmol) were added to the reactor. For the specific example, polymerization was stopped after 2 hours. Final yield after fractionation was 0.43 g (molar composition of DMAA, F_{DMAA} = 0.73) with $\overline{M_n}$= 19.9 kg mol^{-1} and $\overline{M_w}/\overline{M_n}$= 2.26, as measured by GPC relative to PMMA standards in DMF solvent at 50 ^{o}C. Copolymer composition determination by NMR is detailed in the characterization section.

TABLE 2 Formulations for chain extension experiments using *N,N*-dimethylacrylamide (DMAA) monomer performed in 50 wt% DMF solution at 110 °C and molecular weight characterization for poly(MAEPYR-*stat*-VBK)-*b*-poly(DMAA) block copolymers.

ID[a]	Macroinitiator ID[a]	$[Macroinitiator]_0$ (mol·L^{-1})	$[DMAA]_0$ (mol·L^{-1})	$[DMF]_0$ (mol·L^{-1})	$M_{n,target,2}$[b] (kg mol^{-1})
MV-8	MV-2	0.015	1.7	10.7	11.3
MV-9	MV-3	0.016	5.0	6.3	30.7
MV-10	MV-5	0.009	4.8	6.5	52.3

[a] Experiments for poly(MAEPYR-stat-VBK) copolymerizations and chain extensions are denoted MV-Z with M representing *N*-(2-methacryloyloxyethyl)-pyrrolidone, V representing 9-(4-vinylbenzyl)-9H-carbazole, and Z representing the experiment number. [b] The target molecular weight, $M_{n,target,2}$, of the second block was calculated according to $M_{n,target,2} = M_m*[m]_0/[macro]_0$, where M_m is the molecular weight of the monomer, $[m]_0$ and $[macro]_0$ are the initial monomer and macroinitiator concentrations, respectively. The target molecular weight, $M_{n,target,block}$ of the final block can be calculated according to $M_{n,target,block} = M_{n,macro} + M_{n,target,2}$, where $M_{n,macro}$ is the molecular weight of the macroinitiator used.

Synthesis of Poly (N-(2-Methacryloyloxyethyl) Pyrrolidone (poly(MAEPYR)) Homopolymer via RAFT Polymerization.

The polymerization was conducted using AIBN as a source of radicals, and CPDTC as a chain transfer agent (CTA) in DMF (50 wt%) at 75°C. The initial ratio of CTA relative to AIBN $[CTA]_0$:$[AIBN]_0$ was 5. AIBN (0.003 g, 0.019 mmol), CPDTC (0.036 g, 0.104 mmol), MAEPYR (2.53 g, 12.83 mmol), and DMF (2.53 g, 34.61 mmol) were added to the reactor. The polymerization was stopped after 2 hours. The final yield was 0.82 g (88% conversion with $\overline{M_n}$ = 10.9 kg mol^{-1} and $\overline{M_w}/\overline{M_n}$ = 1.60).

Characterization

Polymer Characterization

Gel Permeation Chromatography (GPC)

The number average molecular weight, $\overline{M_n}$, and the dispersity, Đ or $\overline{M_w}/\overline{M_n}$, were determined by gel permeation chromatography (GPC, Water Breeze). GPC was equipped with ultra-violet (UV 2487) and differential refractive index (RI 2414) detectors. The GPC was equipped with 2 ResiPore (3 µm, MULTI pore type, 250 mm x 4.6 mm) columns with a ResiPore guard column (3 µm, 50 mm x 4.6 mm) from Polymer Laboratories. HPLC grade DMF was used as a mobile phase with a flow rate of 0.3 ml min^{-1}. The GPC was calibrated using poly(methyl methacrylate) standards in DMF at 50 °C.

Nuclear Magnetic Resonance Spectroscopy (NMR)

All ^{1}H NMR spectroscopy were performed in $CDCl_3$ using a 400MHz Varian Gemini. Conversion of the MAEPYR was determined by comparing the area associated to the vinyl peaks

(Figure 1) ($H_{1,2}$ δ = 6.08 and 5.56 ppm) to the area associated to the ethyl spacer hydrogens ($H_{3,4}$ δ = 4.0 for the polymer and δ = 4.25 ppm for the monomer). Conversion of the VBK was determined by comparing the areas associated to the vinyl peaks ($H_{5\text{-}7}$ δ = 6.6, 5.7, and 5.2 ppm) to the area associated to the methylene hydrogens ($H_{8,9}$ δ = 5.5 ppm for the monomer and δ = 5.4 ppm for the polymer). Conversion, *X*, of the poly(MAEPYR-stat-VBK) copolymerizations was calculated from $X=X_{MAEPYR}\,\omega_{MAEPYR,0} + X_{VBK}\,\omega_{VBK,0}$, where $\omega_{MAEPYR,0}$ and $\omega_{VBK,0}$ are the initial weight fractions of MAEPYR and VBK, respectively.

The final composition of the statistical and/or block copolymers was determined by the ratio of the ethyl spacer protons corresponding to MAEPYR units ($H_{3,4}$, 2H, δ = 4.0), the methylene protons corresponding to VBK units ($H_{8,9}$, 2H, δ = 5.4 ppm), and the methyl protons corresponding to DMAA units (C-N(CH_3)$_2$, 6H, δ = 3.0 - 3.2 ppm,). For instance, $F_{DMAA} = \frac{I_{DMAA}/6}{I_{MAEPYR}/2+I_{VBK}/2+I_{DMAA}/6}$, where I_{DMAA}, I_{MAEPYR}, I_{VBK} are the integrated areas corresponding to DMAA, MAEPYR, VBK polymer peaks, respectively, and F_{DMAA} is the DMAA composition in the final block copolymer.

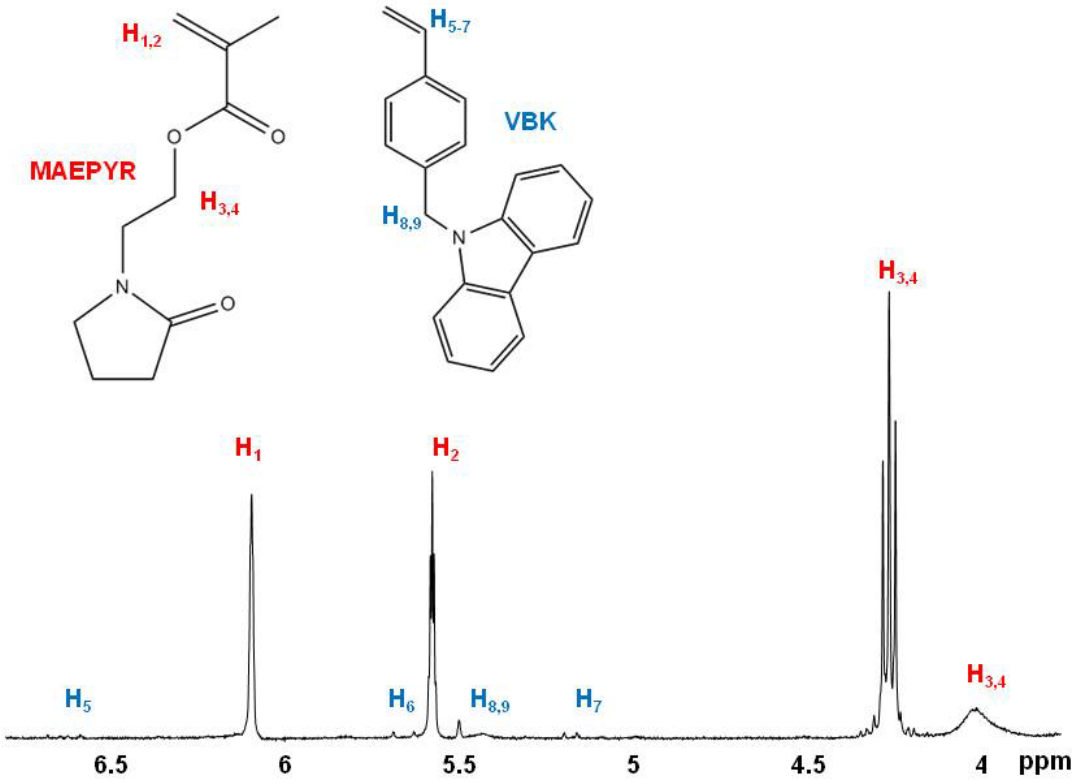

FIGURE 1 Typical ^{1}H NMR ($CDCl_3$) spectra of the crude mixture during a poly(MAEPYR-*stat*-VBK) statistical synthesis. The region shown is only where the peaks used for conversion determination occurred. Note that the peak due to the DMF solvent (~ 3 ppm) is not shown in the region of interest. Also, the aromatic protons due to the carbazole ring are at higher chemical shifts.

^{31}P NMR spectroscopy of isolated poly(MAEPYR-stat-VBK) copolymers was recorded in $CDCl_3$ solvent using a 200MHz Varian Gemini. The copolymer was carefully weighed and a known amount of diethyl phosphate (DEP) was added as an internal standard. The ratio of SG1-capped chains to DEP was calculated using the peaks corresponding to SG1 group (δ = 24 - 27 ppm), and DEP (δ = 8 – 9 ppm). This ratio was compared to the molar ratio of copolymer to DEP to obtain the molar percentage of SG1-capped chains in the sample.

CPT measurement

Two techniques were used to report cloud point temperature (CPT) of a polymer in aqueous solution: UV-Vis spectroscopy and dynamic light scattering (DLS).

UV-Vis spectroscopy

The cloud point temperatures (CPTs) were measured by UV-Vis spectroscopy using a Cary 5000 UV−Vis−NIR spectrometer (Agilent Technologies) equipped with a temperature controlled Peltier thermostatted (6 × 6) multicell holder. The light absorbance was measured at a wavelength of 500 nm. The heating rate and temperature range observed varied from one analysis to another, as these variables were studied. The CPT was determined as the temperature at which the normalized absorbance reached 0.5 on a heating cycle.

Dynamic Light Scattering (DLS)

The Malvern Zetasizer Nano ZS equipped with a 633 nm red laser was used. The samples were filtered using a 0.2 micron filter and then heated in increments of 0.2 °C, allowed to equilibrate for 1 min followed by 10-14 measurements, which were averaged together to give one value at the corresponding temperature. All DLS measurements were performed at a scattering angle (θ) of 173°. For more accurate measurement of the hydrodynamic radius, the refractive index (RI) of a sample has to be estimated. The RI that was used was that of PMMA.

RESULTS AND DISCUSSION

Statistical Copolymer Synthesis

The homopolymerization of methacrylates like MAEPYR using NMP is problematic due to the high equilibrium constant (K) between the dormant and active species, resulting in irreversible termination due to β-hydrogen transfer from the propagating radical to the nitroxide[50]. Recently, NMP of methyl methacrylate (MMA) without any comonomer was successful up until 60% conversion by using a new alkoxyamine based on 2,2-diphenyl-3-phenylimino-2,3-dihydroindol-1-yloxyl (DPAIO) nitroxide[51] with final dispersity close to 1.3 - 1.4. Grubbs and co-workers used *N*-phenylalkoxyamines to homopolymerize MMA up to moderate conversions (up to 50%) while maintaining narrow molecular weight distributions throughout the entire reaction (dispersity of 1.12 - 1.30)[52]. In this study, a commercially available initiator, BlocBuilder, and a controlling comonomer, VBK, are used to yield MAEPYR-rich copolymers. The characteristic plots of the number average molecular weight $\overline{M_n}$ and dispersity $\overline{M_w}/\overline{M_n}$ versus conversion, X, shows a plateau in $\overline{M_n}$ and a significant increase in $\overline{M_w}/\overline{M_n}$ (Figure 2).

The first attempt to copolymerize MAEPYR with as little as 2 mol% VBK (MV- 1, Table 1) with a target molecular weight at complete conversion of 25 kg mol^{-1} resulted in a relatively fast polymerization, reaching 88% conversion in 5 hours. It followed first-order kinetics in the initial stages (Figure 2a) with a noticeable termination at later stages of the polymerization. NMR analysis revealed that at 30 minutes of the reaction, about 80% of VBK monomer (VBK_m) was polymerized (Figure 3). With almost no controlling comonomer remaining in the mixture, the propagation rates increased drastically and increased the probability of irreversible termination reactions[42]. The number average molecular weight of MV-1 versus conversion is

linear in Figure 2c. The Đ increased at the early stage of polymerization and then decreased steadily to 1.58 at the final conversion of 88%.

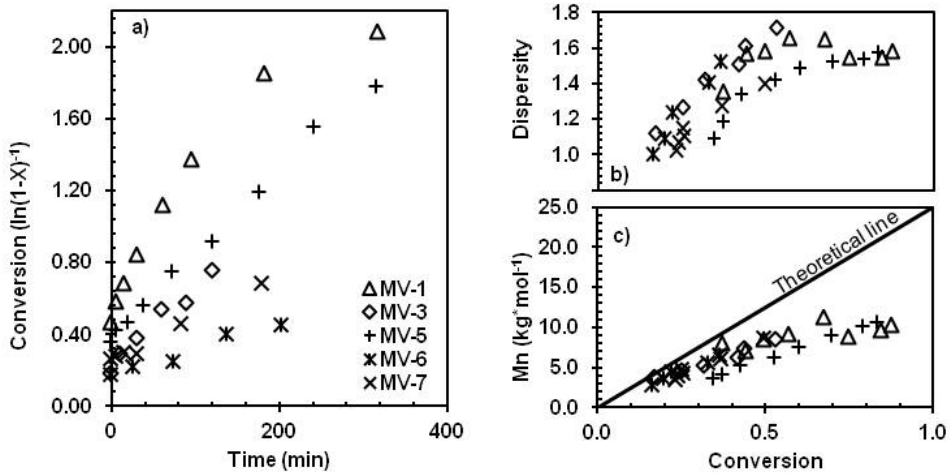

FIGURE 2 a) The semi-logarithmic plots of scaled conversion ($\ln[1-X]^{-1}$]) (X = conversion) versus time; b) the dispersity, Đ, versus X plots; c) the number average molecular weight ($\overline{M_n}$) versus X plots for poly(MAEPYR-*stat*-VBK) copolymerizations at varying VBK feed content, where the symbols are as follows: Δ ($f_{VBK,0}$ = 0.02); ◊ ($f_{VBK,0}$ = 0.04); + ($f_{VBK,0}$ = 0.05); * ($f_{VBK,0}$ = 0.08); x ($f_{VBK,0}$ = 0.10).

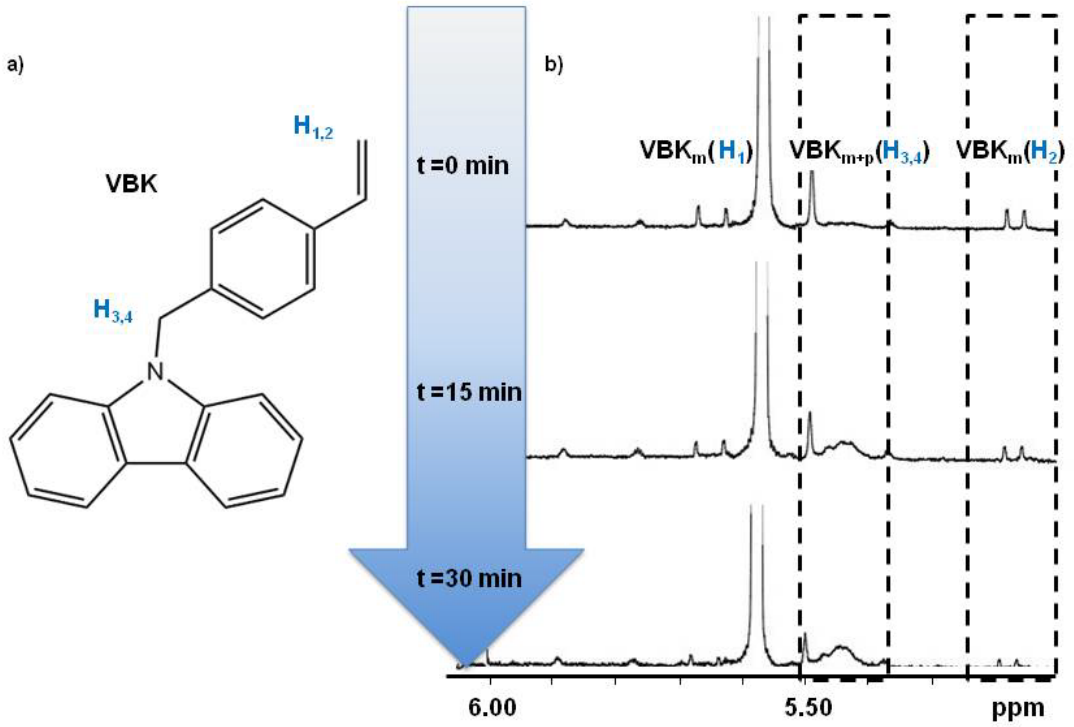

FIGURE 3 a) Labeled protons (H_{1-4}) of 9-(4-vinylbenzyl)-9H-carbazole monomer (VBK_m) and the corresponding ^1H NMR spectra are shown in b) for MV-1 in $CDCl_3$ at various polymerization times. VBK_m are the peaks corresponding to monomer only, and VBK_{m+p} are the peaks corresponding to both monomer and polymer.

Based on the results presented in Figure 2, it showed that the initial concentration of VBK clearly influenced the control of the polymerization. Table 1 shows all the formulations studied. Characteristic kinetic plots for poly(MAEPYR-stat-VBK) copolymerizations with various VBK compositions are shown in Figure 2. The polymerization rate, as indicated by the slope, decreased with increasing VBK initial feed composition. Number average molecular weight ($\overline{M_n}$) increased linearly with conversion up to 60 – 80 % with final copolymers characterized by monomodal molecular weight distributions even though dispersities were somewhat high (Đ < 1.7). The molecular weight data did not follow the theoretical line precisely

(Figure 2c) for two reasons likely. First, the difference in hydrodynamic volume of the samples and the PMMA standards used for the GPC calibration could be the source for the difference. Second, the deviations from the theoretical line at higher conversions might be due to the presence of irreversible termination reactions. The properties of the final statistical copolymers are listed in Table 3. At t = 0 in Figure 2, there are conversions 24 % - 38 %, which suggests that fast polymerization occurred during the initial stage. BlocBuilder begins to decompose at much lower temperatures[53] compared to the reaction temperature, and it would initiate the reaction before the set point temperature, which was taken as t = 0. The heating rate was set so that the set point temperature is reached within 10 - 15 minutes so as to minimize the polymerization rate before the prescribed set point was attained. It is interesting to note that in almost all the cases, the controlling comonomer, VBK, was consumed faster than the methacrylate monomer (MAEPYR), which explains the higher VBK content in the final polymer when compared to the initial feed composition. Only for the case of MV-1 is the composition much richer in methacrylate than expected.

TABLE 3 Molecular weight characterization for poly(MAEPYR-stat-VBK) statistical copolymers.

ID[a]	Symbol	$M_{n,target}$ (kg mol^{-1}) [b]	$f_{VBK,0}$[c]	F_{VBK}[c]	X[d]	M_n (kg mol^{-1})[e]	M_w/M_n[e]
MV-1	Δ	24.8	0.02	0.01	0.88	10.2	1.58
MV-2	○	10.0	0.04	0.05	0.76	5.9	1.43
MV-3	◊	25.2	0.04	0.06	0.53	8.4	1.71
MV-4	□	49.3	0.04	0.06	0.59	24.1	2.32
MV-5	+	24.9	0.05	0.06	0.83	11.8	1.56
MV-6	*	25.8	0.08	0.16	0.37	8.5	1.59
MV-7	x	24.9	0.10	0.16	0.80	10.3	1.56

[a] Experiments for poly(MAEPYR-stat-VBK) copolymerizations are denoted MV-Z with M representing *N*-(2-methacryloyloxyethyl)-pyrrolidone, V representing 9-(4-vinylbenzyl)-9H-carbazole, and Z representing the experiment number; [b] The target molecular weight was

calculated according to equation 1; [c] $f_{VBK,0}$ is the initial molar fraction of VBK in the feed; F_{VBK} is the molar fraction of VBK in the final copolymer as determined by ^{1}H NMR spectroscopy; [d] Monomer conversion determined by ^{1}H NMR spectroscopy; [e] Number-average molecular weight ($\overline{M_n}$) and dispersity were determined by GPC.

Figure 4 shows the effect of different target molecular weights on the kinetics, while keeping the initial feed composition of the controlling comonomer constant. The theoretical molecular weight depends on the alkoxyamine concentration[42, 54] and can be calculated by Equation 1.

$$M_n = M_I + \frac{[m]_0}{[I]_0} \cdot X \cdot M_m \qquad \text{(Equation 1)}$$

In Equation 1, M_n is the target molecular weight of the final polymer at complete conversion (X = 1); M_I and M_m are the molecular weight of the initiator and monomer, respectively; $[m]_0$ and $[I]_0$ are the initial monomer and initiator concentrations, respectively.

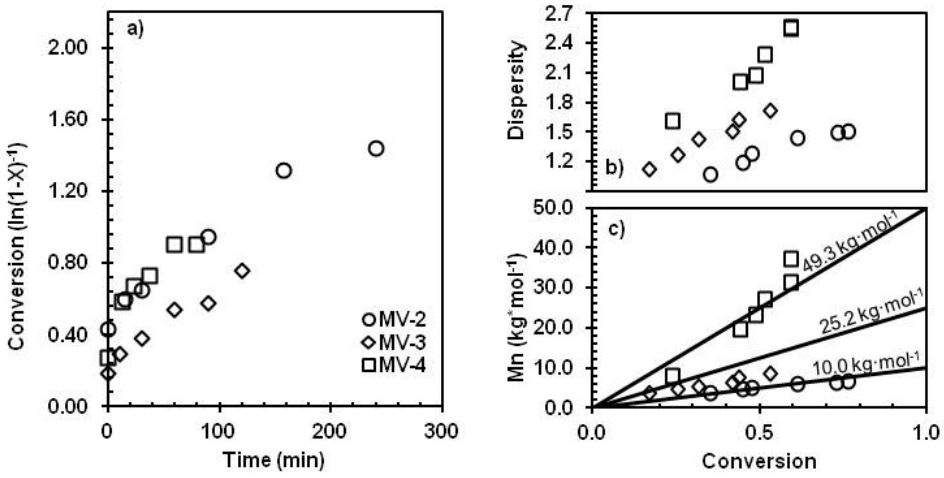

FIGURE 4 a) The semi-logarithmic plots of scaled conversion ($\ln[1\text{-}X]^{-1}$]) (X = conversion) versus time; b) the dispersity, Đ, versus X plots, and c) the number average molecular weight ($\overline{M_n}$) versus X plots for poly(MAEPYR-stat-VBK) copolymerizations at varying target molecular weight, where ○ ($M_{n,target}$ = 10.0 kg mol^{-1}); ◊ ($M_{n,target}$ = 25.2 kg mol^{-1}); □ ($M_{n,target}$ = 49.3 kg mol^{-1}).

For low target molecular weight, there is sufficiently high alkoxyamine concentration in the solution, and the persistent radical effect (PRE)[42] helps to control the reaction by decreasing the polymerization rate. As the result, the final polymers are characterized by relatively narrow molecular weight distribution (Đ ~ 1.4, Figure 4b). In contrast, at low alkoxyamine solution concentration, the PRE is less profound. The polymerization rates are high, and the probability of termination reactions increases, which is exemplified by a broad molecular weight distribution (Đ ~ 2.5, Figure 4b). Number average molecular weights for all three experiments in Figure 4 increased linearly with conversion up to approximately 60% conversion.

A typical set of GPC chromatograms for the poly(MAEPYR-*stat*-VBK) statistical copolymerizations is shown in Figure 5a, whereas Figure 5b shows GPC traces for chain extension experiments with DMAA. The growth of the chains with time in both cases is indicated by the shift of the peaks in the chromatogram to lower elution times (higher molecular weight). The tailing on the low molecular weight side is likely due to irreversible termination.

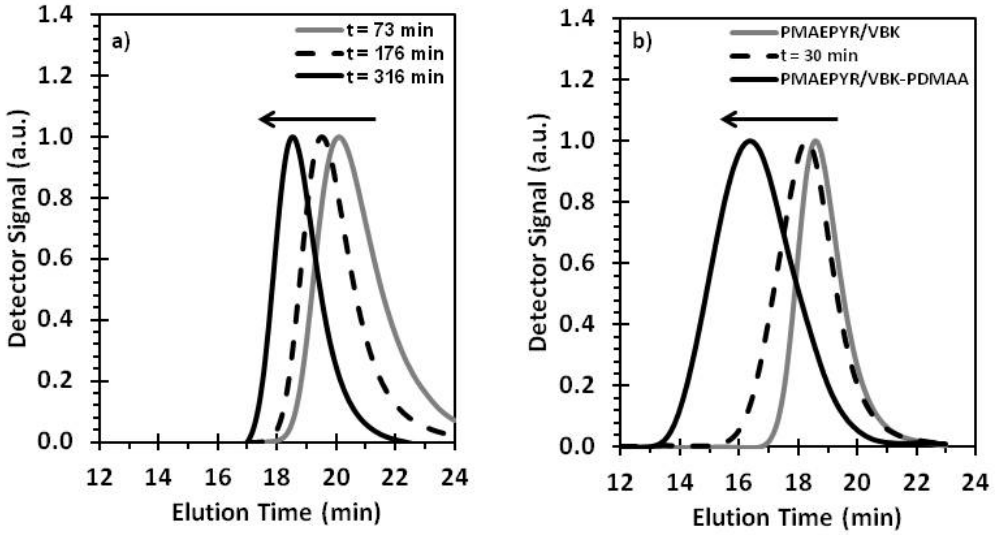

FIGURE 5 Gel permeation chromatograms (GPC) of a) a characteristic copolymerization of MV-5; b) DMAA chain extension (MV-10) done in a 50 wt% solution in DMF at 110°C from MV- 5 macroinitiator.

2.2 Block Copolymer Synthesis

To test the ability of the final polymers to reinitiate a fresh batch of monomer, chain extension experiments were performed with DMAA monomer in DMF solvent (Scheme 1). The formulations for all the chain extension experiments are listed in Table 2. The monomodal shift in the GPC chromatograms (Figure 5b) for MV-10 suggests that the macroinitiator (MV-5) was significantly SG1-terminated. Similar behavior was observed for the other two chain extension experiments (MV-8 and MV-9). Table 4 lists the properties of all final block copolymers. The dispersity values of the final chain-extended samples are quite high, which is suggestive of poor re-initiation. Fractionation was attempted to separate the dead chains from the block copolymer, but with little success; however, the DMAA content in the final polymer decreased slightly (for instance, F_{DMAA} = 0.73 for MV-9 after the fractionation and 0.90 before the fractionation). ^{31}P NMR spectroscopy was used to determine the amount of SG1 present at the chain ends (since phosphorus is present in SG1[53]). For instance, it was found that MV-2 was 13 % living. Such a low fraction of SG1-terminated chains explained the poor re-initiation and broad dispersities of the final block copolymers. However, ^{31}P NMR spectroscopy might be misleading since the concentration of phosphorus in the polymer was very low and could lead to substantial error.[44, 55] The GPC chromatograms of the chain extensions shown in Figure 5 did not indicate an obvious peak corresponding to unreacted macroinitiator; this may be due to the molecular weights/hydrodynamic volumes of the species not being very different from one another.

TABLE 4 Molecular weight characterization for poly(MAEPYR-stat-VBK)-b-poly(DMAA) block copolymers.

ID[a]	Macroinitiator ID[a]	Macroinitiator M_n[b] (kg mol^{-1})	Macroinitiator M_w/M_n[b]	M_n[b] (kg mol^{-1})	M_w/M_n[b]	F_{DMAA}[c]
MV-8	MV-2	5.9	1.43	12.4	2.37	0.92
MV-9	MV-3	8.4	1.71	19.9	2.26	0.73
MV-10	MV-5	11.8	1.56	53.5	2.96	0.89

[a] Experiments for poly(MAEPYR-stat-VBK) copolymerizations and chain extensions are denoted MV-Z with M representing *N*-(2-methacryloyloxyethyl)-pyrrolidone, V representing 9-(4-vinylbenzyl)-9H-carbazole, and Z representing the experiment number; [b] Number-average molecular weight ($\overline{M_n}$) and dispersity index were determined by GPC; [c] F_{DMAA} is the molar fraction of DMAA in the final block copolymer as determined by ^{1}H NMR spectroscopy.

2.3 Solution properties of statistical and block copolymers

The MAEPYR-rich statistical copolymers and block copolymers were tested for thermo-responsive behaviour in aqueous media. Properties of stimuli-responsive polymers are connected to the microstructure of the polymer; therefore, well-defined polymers with narrow molecular weight distributions are essential for clear determination of CPT.[18, 27-29] Davis and co-workers synthesized MAEPYR homopolymers via conventional polymerization.[41] Although there is no information given about the microstructure of the resulting polymers, the CPTs in water (0.7 wt%) were measured at a heating rate of 1°C min^{-1} and the CPTs ranged between 29 - 34 °C[41]. Cai et al. reported CPTs of 2 wt% solutions ranging from 52.8 - 71.5 °C for MAEPYR homopolymers synthesized by RAFT polymerization with weight-average molecular weights of 105.4 to 20.6 kg mol^{-1}, respectively[40]. Here, the effect of composition, solution concentration and heating rate on CPT was studied.

2.3.1 Effect of composition on the transition of statistical copolymers.

Poly(MAEPYR-stat-VBK) statistical copolymers exhibited tuneable cloud point temperature (CPT) by varying VBK content. Increasing the content of the more hydrophobic monomer, VBK, in the final copolymer structure will decrease the CPT due to the decreased

degree of hydrogen bonding with water.[7, 56, 57] Poly(MAEPYR) homopolymer (see experimental section for details about the synthesis and characterization) has a CPT of 59.0 °C ($\overline{M_n}$= 10.9 kg mol^{-1}), and the CPT decreased to 49.7 °C (for MV-1 with F_{VBK} = 1 mol%, $\overline{M_n}$ = 10.2 kg mol^{-1}) and 39.6 °C (for MV-5 with F_{VBK} = 6 mol%, $\overline{M_n}$ = 11.8 kg mol^{-1}) for poly(MAEPYR-stat-VBK) statistical copolymers at 1 wt% solution concentration. Poly(MAEPYR) homopolymer ($\overline{M_n}$= 10.9 kg mol^{-1}) has a CPT of 53.5 °C at 2 wt%, which is slightly different from the values reported by Cai (71.5 °C at 20.6 kg mol^{-1}) at the same concentration. The difference may arise from different polymer samples used (e.g. molecular weight is relative to either PMMA or PS standards, for this and Cai's work, respectively), due to higher dispersity values associated with polymers used in this work (compared to Đ of 1.11-1.13 for polymers used in Cai's work) and/or due to the conditions used for the CPT determination (e.g. heating rates, and turbidity versus light scattering methods).

2.3.2 Effect of solution concentration on the transition of statistical copolymers.

Particle size was measured by dynamic light scattering (DLS, see the experimental section) for the statistical copolymers during the phase transition. poly(MAEPYR-*stat*-VBK) statistical copolymers with low VBK content (e.g. MV-1) were readily soluble at room temperature in deionized water. The light scattering intensity was low, as measured by DLS, from room temperature until about 39 ºC (Figure 6a). During heating, the intensity increased significantly when the temperature reached the critical temperature, which is the CPT.[20] From Figure 6a it is seen that the intensity increased dramatically at 42 °C. The intensity is related to the particle size: larger particles scatter light more, which would result in higher intensity[58]. Hence, it is possible to determine the CPT by monitoring the change in the population of particle sizes. Figures 6c and 6b show the temperature dependence of average hydrodynamic radius,

466 $\langle R_h \rangle$, of poly(MAEPYR-*stat*-VBK) chains (MV-1, $\overline{M_n}$= 10.2 kg mol^{-1}, F_{VBK} = 0.01) in one
467 heating cycle as measured by DLS, and normalized absorbance of the heating ramp of the same
468 sample as measured by UV-Vis spectroscopy, respectively. The CPT at 50 % normalized
469 absorbance is 49.7 ºC and 40.9 ºC for 0.5 and 1 wt% solutions, respectively, and the $\langle R_h \rangle$
470 increased at a temperature above 47 and 42 °C, respectively. The $\langle R_h \rangle$ measurements showed
471 considerable scatter above the CPT, which is likely due to sedimentation.[40] The CPT by DLS
472 was determined when the intensity-weighted particle distribution was shifted from the lower to
473 the higher $\langle R_h \rangle$ as indicated in Figure 6a. The transparent solution became opaque when the
474 temperature was above the CPT due to aggregation[20, 59] of polymer chains. The temperature-
475 induced phase separation was reversible, and the polymer solution became clear again when the
476 temperature was below the CPT.

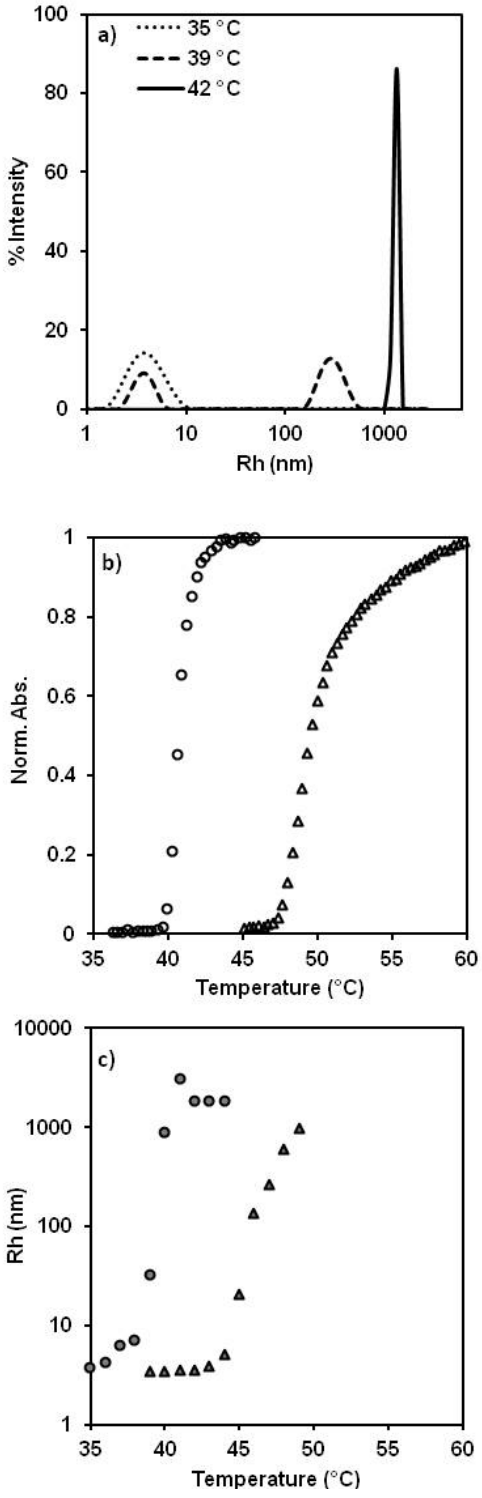

477

478 FIGURE 6 a) The distribution of different particle size populations during DLS measurement of
479 statistical poly(MAEPYR-*stat*-VBK) copolymer MV-1 ($\overline{M_n}$ = 10.2 kg mol^{-1}, Đ = 1.58, F_{VBK} =
480 0.01) at 1 wt% solution during a heating ramp; b) The normalized absorbance as measured by

UV-Vis and c) average hydrodynamic radius (<R_h>) as measured by DLS of MV- 1 at 0.5 wt% solution (triangles) and 1 wt% solution (circles) during one heat cycle.

At lower solution concentration (Figure 7) the CPT increases since the formation of polymer aggregates is a much slower process at low polymer concentrations[59]. Depending on the solution concentration, MV-1 exhibited a difference of as much as 16.6 °C in CPTs (from 50.9 °C for 0.3 wt% solution to 34.3 °C for 4 wt% solution). These observations are consistent with literature.[19, 59-62] For instance, the CPT for poly(DMAEMA-*stat*-styrene) copolymers decreased by 7 - 10 °C when the solution concentration increased from 0.1 to 0.3 wt%.[60] Similarly, PNIPAM polymer samples showed a significant concentration dependence below 5 wt%, and the curve reaches a plateau at higher concentrations (15-20 wt%).[59] The polymer samples, other than MV-1 and MV-5, were water-insoluble, and were not considered for the analysis.

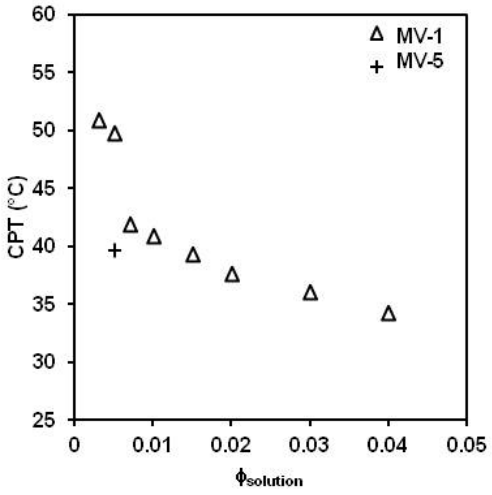

FIGURE 7 CPT dependence of MV-1 (Δ, $\overline{M_n}$ = 10.2 kg mol^{-1}, Đ = 1.58, F_{VBK} = 0.01) and MV-5 (+, $\overline{M_n}$ = 11.8 kg mol^{-1}, Đ = 1.56, F_{VBK} = 0.06) samples on composition and MV-1 samples on solution concentration as measured by UV-Vis spectroscopy with a heating ramp of 1 °C min^{-1}.

2.3.3 Hysteresis and effect of scanning rate on the transition of statistical copolymers.

One of the most important properties of "smart" polymers is the reversibility of the phase transition. It was found that the temperature-induced phase separation was reversible, but the hysteresis effect was noticeable since the temperature of the phase transition in the cooling process was different from the one in the heating process. The hysteresis observed was as low as 2 °C and as high as 10 °C when the rate of heating and cooling was 1 °C min^{-1}. Cai et al. reported no profound hysteresis effect for one heating-cooling cycle for one of the many poly(MAEPYR) homopolymers they examined ($\overline{M_w}$ = 105.4 kg mol^{-1})[40]. In our study, the $\overline{M_n}$s of the copolymers studied were 10.2-11.8 kg mol^{-1} (relative to PMMA standards) and the hysteresis effect becomes larger as the molecular weight decreases: smaller chains tend to form larger aggregates due to interchain association, which are more difficult to dissociate during the cooling cycle due to the increased degree of hydrogen bonding.[17, 62] It is interesting to note that the poly(MAEPYR) homopolymer (synthesized by RAFT for comparison, see experimental section) exhibited very little hysteresis of 2 °C when observed under the same conditions (1 wt% solution, heating/cooling rate of 1 °C min^{-1}) as MV-1 copolymer. The observed difference for our samples suggests the presence of weak van der Waals interactions[18] and/or hydrophobic interactions of the polymer's backbone with the ethyl spacers and the carbazole groups from the VBK comonomer.

The CPT strongly depends on the heating rate[57, 59, 63]. As the heating rate was increased, the CPT for MV-1 samples at 1 wt% concentration was found to increase as well. For example, the CPT increased from 39.8 °C to 45.2 °C for the heating rates ranging from 0.2 to 4 °C min^{-1}, respectively. Similar behavior was observed previously in other systems.[19, 59, 63] For instance, increasing the heating rate from 0.02 to 5 °C min^{-1} resulted in about 11 °C increase in CPT for

PNIPAM, as determined by turbidity methods.[59] Poly(*N*,*N*-diethylacrylamide) (DEAAM) showed only a 6 °C increase in CPT when the heating rate was altered from 0.06 to 5°C min^{-1}.[63] Polymer-polymer interactions responsible for the phase separation are time-dependent and at higher heating/cooling rates there is less time to react to the environmental change.[57, 63] As a result, the transitions become more diffusive[19, 63], with a partial loss of reversibility[19]. For very high heating rates (3 - 4 °C min^{-1}), the transition of MV-1 samples during the cooling process was very broad, and the solution became clear only at room temperature.

2.3.4 Transition of block copolymers.

For the poly(MAEPYR-stat-VBK) statistical copolymers, CPT was tuned by the inclusion of the more hydrophobic monomer, VBK, which resulted in lower CPTs as VBK content increased. It is possible to tune CPT in the opposite direction by chain-extending the copolymer with a hydrophilic monomer. Many water-soluble monomers are polymerizable by NMP, including *N*,*N*-dimethylacrylamide (DMAA)[64], *N*-vinylpyrrolidone (VP)[23], 2-*N*-morpholinoethyl acrylate (MEA)[19] and 4-acryloylmorpholine (4AM)[65]. In this study, DMAA was used in the synthesis of a hydrophilic block. With the temperature changes, the block copolymer might gain or lose its amphiphilicity, resulting in formation or dissolution of micelles.[7] There are two types of micelles that can be formed. One type consists of the temperature responsive corona, and the other one has the temperature responsive inner core. In the case of poly(MAEPYR-*stat*-VBK)-*b*-poly(DMAA) block copolymers, the hydrophilic DMAA block would form the outer shell, and the inner core would consist of the temperature responsive copolymer resulting in stable micelle formation below the LCST.[45] Figure 8 shows the temperature dependence of average hydrodynamic radius, $\langle R_h \rangle$, of poly(MAEPYR-*stat*-VBK)-*b*-poly(DMAA) chains (MV-8 and MV-9) in one heating cycle as measured by DLS, and

544 normalized absorbance on the heating ramp of the same sample as measured by UV-Vis
545 spectroscopy. The increase of average size near the CPT suggests the presence of intermicellar
546 aggregation[66], which is minimal due to the hydrophilic poly(DMAA) block. As a result, the final
547 average hydrodynamic radius for the block copolymer is smaller than that of the statistical
548 copolymers.[45] Also, above the LCST, the hydrophobic effect in the core might disappear due to
549 the interactions of the hydrophilic block, if it is too long, resulting in micelle destruction.[7]
550 Addition of the hydrophilic poly(DMAA) block slowed the rate of phase transition for the block
551 copolymers, compared to the statistical copolymers. From Figure 8 it is seen that the phase
552 transition observed by UV-Vis spectroscopy occurs over several tens of degrees (45 - 85 °C for
553 MV-8 chains, for example). Similar behavior was observed in the literature.[45, 66] Dispersity of the
554 final polymer influenced the phase transition as well. Smaller chains tend to form larger
555 aggregates due to additional hydrogen bonding present in the interchain associations, whereas
556 larger chains are likely to undergo only intrachain contractions.[17] The two types of interactions
557 do not occur simultaneously. With the broad molecular weight distributions (for example, Đ =
558 2.26 - 2.96 for MV-8, MV-9, MV-10 polymers) the transition will become more diffuse as a
559 result of the difference in time required to form aggregates for chains of different length.
560 As predicted, the hydrophilic monomer shifted the CPT upwards, if compared to the CPT
561 of the precursor MV-1. The CPTs of the macroinitiators (MV-2 and MV-3 in this case) were not
562 determined due to limited solubility of the polymer in aqueous solution. The final CPTs for block
563 copolymers as determined by UV-Vis spectroscopy and DLS are summarized in Table 5. There
564 is a discrepancy between the determined CPT values, which is solely due to the analytical
565 technique used. UV-Vis spectroscopy relies on turbidity measurements, so it is sensitive only to
566 the macroscopic phase separation, which is a slow process at low solution concentration.[59] DLS,

on the other hand, can detect the collapse of a single polymer chain[59], before the macroscopic phase separation, which occurs usually at a higher temperature. From Figure 8 it is seen that the transition, as determined by DLS, is sharper than the one determined by UV-Vis; therefore, CPT values for block copolymers were reported from the DLS measurements.

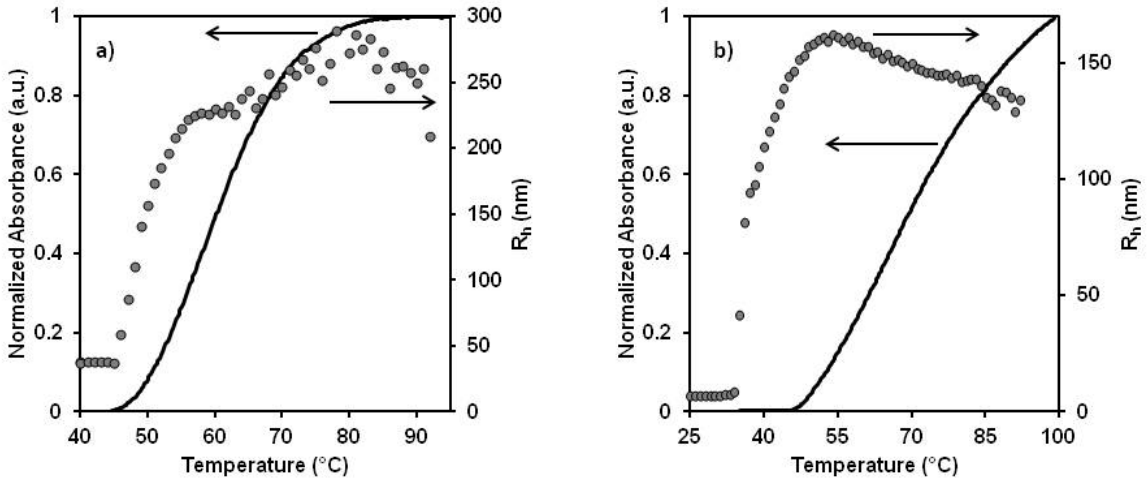

FIGURE 8 Temperature dependence of the normalized absorbance (black line) as measured by UV-Vis during the heat cycle and average hydrodynamic radius (<R_h>) (grey circles) as measured by DLS during the heat cycle of a) MV-8 chains ($\overline{M_n}$= 12.4 kg mol^{-1}, Đ = 2.37, F_{DMAA} = 0.92); b) MV-9 ($\overline{M_n}$ = 19.9 kg mol^{-1}, Đ = 2.26, F_{DMAA} = 0.73), both in 1 wt% solution.

TABLE 5 The difference in the CPTs for poly(MAEPYR-stat-VBK)-b-poly(DMAA) block copolymers as determined by UV-Vis spectroscopy and DLS, and the corresponding CPT values determined on a heating ramp.

ID[a]	Macroinitiator ID[a]	CPT by UV-Vis (°C)	CPT by DLS (°C)	$\phi_{solution}$ (wt%)
MV-8	MV-2	60.3	50	1
MV-9	MV-3	69.4	39	1
MV-10	MV-5	82.9	48	1
MV-10	MV-5	66.2	n/a	2

[a] Experiments for poly(MAEPYR-stat-VBK) copolymerizations and chain extensions are denoted MV-Z with M representing *N*-(2-methacryloyloxyethyl)-pyrrolidone (MAEPYR), V

representing 9-(4-vinylbenzyl)-9H-carbazole (VBK), and Z representing the experiment number. Composition and molecular weight data of the final blocks can be found in Table 4.

2.3.5 Stability of statistical and block copolymers.

The stability of the phase transition was tested by observing the changes in particle size over a prolonged period of time. The 1 wt% solutions of statistical and block copolymers, MV-1 and MV-10, respectively, were held above the CPT at 50 °C for 15 hours (Figure 9). The changes in $<R_h>$ for MV-1 over the 15-hour period indicated that the system was not stable. At the end of the experiment, the polymer settled at the bottom of the vial, which suggested that macrophase separation had occurred[18]. In contrast, the changes in $<R_h>$ are less profound for MV-10, indicating that the micelles formed were relatively stable.

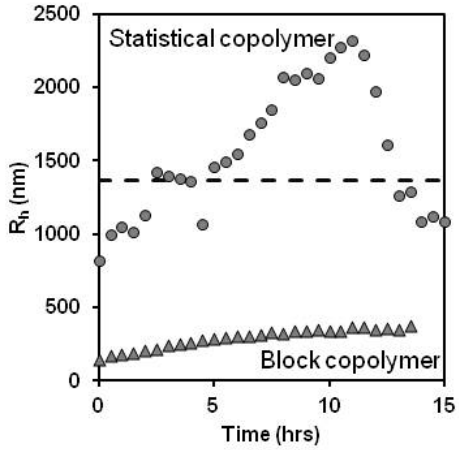

FIGURE 9 Time dependence of the average hydrodynamic radius ($<R_h>$) of 1 wt% statistical copolymer (MV-1, $\overline{M_n}$ = 10.2 kg mol^{-1}, Đ = 1.58) and block copolymer (MV-10, $\overline{M_n}$ = 53.5 kg mol^{-1}, Đ = 2.96) solutions at a constant temperature of 50 °C.

Conclusion

The BlocBuilder/SG1 initiators were able to copolymerize MAEPYR-rich compositions in a relatively controlled manner with a minimum of 5 mol% VBK in the initial feed to give linear number average molecular weight $\overline{M}_n$ versus conversion (until about 60% conversion) with fairly narrow molecular weight distributions of the final polymers (dispersity of 1.4 - 1.7). The ability of the final copolymers to reinitiate a fresh monomer batch was tested using DMAA monomer. In all cases studied, the growth of the polymer chains was monitored via GPC, where a shift of the peak to a lower elution time indicated the increase in molecular weight. The final statistical and block copolymers were tested for LCST-type behavior in aqueous solutions. The effect of VBK composition shifted the CPT from 49.7 °C (for MV-1 with $\overline{M_n}$ = 10.2 kg mol^{-1} and F_{VBK} = 0.01) to 39.6 °C (for MV-5 with $\overline{M_n}$ = 11.8 kg mol^{-1} and F_{VBK} = 0.06) at 1 wt% solution concentration. The CPT also decreased with increasing solution concentration, and MV-1 exhibited a difference of as much as 16.6 °C in CPTs (from 50.9 °C for 0.3 wt% solution to 34.3 °C for 4 wt% solution). The CPT was found to be a function of the heating/cooling rate, and the transitions became more diffusive in nature at higher rates. For the block copolymers, the particle size measurements indicated the block copolymers had a broader transition compared to statistical copolymers and that the block copolymer micelles were relatively stable upon prolonged heating above the CPT.

Acknowledgement

The authors are very grateful for the funding support from the NSERC Discovery Grant and the Eugenie Ulmer Lamothe (EUL) Scholarship. The authors also thank Prof. Bruce Lennox for the use of his UV-Vis spectrometer. Finally, the authors thank Arkema, Inc. for help in obtaining BlocBuilder (Mickael Havel) and SG1 (Noah Macy).

References

1 B. Jeong, A. Gutowska, *Trends Biotechnol.* **2002**, *20*, 360-360.
2 T. Okano, *Adv. Polym. Sci.* **1993**, *110*, 179-197.
3 B. R. Twaites, C. D. Alarcon, D. Cunliffe, M. Lavigne, S. Pennadam, J. R. Smith, D. C. Gorecki, C. Alexander, *J. Controlled Release* **2004**, *97*, 551-566.
4 D. Roy, J. N. Cambre, B. S. Sumerlin, *Prog. Polym. Sci.* **2010**, *35*, 278-301.
5 N. Lomadze, H. M. Schneider, *Tetrahedron Lett.* **2005**, *46*, 751-754.
6 C. D. H. Alarcon, S. Pennadam, C. Alexander, *Chem. Soc. Rev.* **2005**, *34*, 276-285.
7 E. S. Gil, S. M. Hudson, *Prog. Polym. Sci.* **2004**, *29*, 1173-1222.
8 A. Chilkoti, M. R. Dreher, D. E. Meyer, D. Raucher, *Adv. Drug Delivery Rev.* **2002**, *54*, 613-630.
9 J. Weidner, *Drug Discovery Today* **2001**, *6*, 1239–1241.
10 M. Yamato, C. Konno, A. Kushida, M. Hirose, M. Utsumi, A. Kikuchi, T. Okano, *Biomaterials* **2000**, *21*, 981–986.
11 K. Uchida, K. Sakai, E. Ito, O. H. Kwon, A. Kikuchi, M. Yamato, T. Okano, *Biomaterials* **2000**, *21*, 923–929.
12 R. J. Young, P. A. Lovell, *Introduction to Polymers*. 3rd ed., CRC Press, Boca Raton, FL, **2011**, pp. 312-314.
13 Y. Maeda, T. Higuchi, I. Ikeda, *Langmuir* **2000**, *16*, 7503-7509.
14 H. Chang, L. Shen, C. Wu, *Macromolecules* **2006**, *39*, 2325-2329.
15 Y. Ding, X. Ye, G. Zhang, *Macromolecules* **2005**, *38*, 904-908.
16 M. Heskins, J. E. Guillet, *J. Macromol. Sci., Part A: Chem.* **1968**, *2*, 1441-1455.
17 Y. C. Tang, Y. W. Ding, G. Z. Zhang, *J. Phys. Chem. B* **2008**, *112*, 8447-8451.
18 J. Sun, Y. Peng, Y. Chen, Y. Liu, J. Deng, L. Lu, Y. Cai, *Macromolecules* **2010**, *43*, 4041-4049.
19 B. H. Lessard, X. Savelyeva, M. Maric, *Polymer* **2012**, *53*, 5649-5656.
20 P. Liu, L. Xiang, Q. Tan, H. Tang, H. Zhang, *Polym. Chem.* **2013**, *4*, 1068-1076.
21 X. Liu, Y. Xu, Z. Wu, H. Chen, *Macromol Biosci.* **2012**, *13*, 147-154.
22 J. Nicolas, Y. Guillaneuf, C. Lefay, D. Bertin, D. Gigmes, B. Charleux, *Prog. Polym. Sci.* **2013**, *38*, 63-235.
23 P. Bilalis, M. Pitsikalis, N. Hadjichristidis, *J. Polym. Sci. Part A: Polym. Chem.* **2006**, *44*, 659-665.
24 H. A. Ravin, A. M. Seligman, J. Fine, *N. Engl. J. Med.* **1952**, *247*, 921-929.
25 U. Karaaslan, M. Parlaktuna, *Prepr. Pap. - Am. Chem. Soc., Div. Fuel Chem.* **2002**, *47*, 355-358.
26 N. Daraboina, P. Linga, *Chem. Eng. Sci.* **2013**, *93*, 387-394.
27 S. Aoshima, H. Oda, E. Kobayashi, *J. Polym. Sci. Part A: Polym. Chem.* **1992**, *30*, 2407-2413.
28 H. Mori, H. Iwaya, A. Nagai, E. T., *Chem. Commun.* **2005**, 4872-4874.
29 P. Liu, H. Xie, H. Tang, G. Zhong, H. Zhang, *J. Polym. Sci. Part A: Polym. Chem.* **2012**, *50*, 3664-3673.
30 K. Matyjaszewski, T. P. Davis, (eds.), *Handbook of Radical Polymerization*. Wiley-Interscience, Hoboken, NJ, **2002**, pp. 920.
31 G. Moad, E. Bicciocchi, M. Chen, J. Chiefari, C. Guerrero-Sanchez, M. Haeussler, S. Houshyar, D. Keddie, E. Rizzardo, S. H. Thang, J. Tsanaktsidis, in *Progress in*

Controlled Radical Polymerization: Mechanisms and Techniques. **2012**, *1100*, pp. 243-258.
32 G. Moad, E. Rizzardo, S. H. Thang, *Acc. Chem. Res.* **2008**, *41*, 1133-1142.
33 G. Moad, J. Chiefari, Y. K. Chong, J. Krstina, R. T. A. Mayadunne, A. Postma, E. Rizzardo, S. H. Thang, *Polym. Int.* **2000**, *49*, 993-1001.
34 G. Moad, R. T. A. Mayadunne, E. Rizzardo, M. Skidmore, S. H. Thang, *ACS Symp. Ser.* **2003**, *854*, 520-535.
35 M. Cunningham, M. Lin, J. A. Smith, J. Ma, K. McAuley, B. Keoshkerian, M. Georges, *Prog. Colloid Polym. Sci. S.* **2004**, *124*, 88-93.
36 R. B. Grubbs, *Polym. Rev.* **2011**, *51*, 104-137.
37 C. J. Hawker, A. W. Bosman, E. Harth, *Chem. Rev.* **2001**, *101*, 3661-3688.
38 K. Matyjaszewski, N. V. Tsarevsky, *Nat. Chem.* **2009**, *1*, 276–288.
39 K. Matyjaszewski, W. A. Braunecker, *Prog. Polym. Sci.* **2007**, *32*, 93-146.
40 J. Deng, Y. Shi, W. Jiang, Y. Peng, L. Lu, Y. Cai, *Macromolecules* **2008**, *41*, 3007-3014.
41 G. M. Iskander, L. E. Baker, D. E. Wiley, T. P. Davis, *Polym. Chem.* **1998**, *39*, 4165-4169.
42 B. Charleux, J. Nicolas, O. Guerret, *Macromolecules* **2005**, *38*, 5485-5492.
43 J. Nicolas, S. Brusseau, B. Charleux, *J. Polym. Sci. Part A: Polym. Chem.* **2010**, *48*, 34-47.
44 B. Lessard, E. J. Ling, M. S. T. Morin, M. Maric, *J. Polym. Sci. Part A: Polym. Chem.* **2011**, *49*, 1033-1045.
45 B. Lessard, M. Maric, *J. Polym. Sci. Part A: Polym. Chem.* **2011**, *49*, 5270-5283.
46 C. Zhang, M. Maric, *J. Polym. Sci. Part A: Polym. Chem.* **2013**, *51*, 4702-4715.
47 B. H. Lessard, E. J. Ling, M. Maric, *Macromolecules* **2012**, *45*, 1879-1891.
48 B. H. Lessard, M. Maric, *Can. J. Chem. Eng.* **2012**, *91*, 618-629.
49 W. Zhang, Y. Yan, N. Zhou, Z. Cheng, J. Zhu, C. Xia, X. Zhu, *Eur. Polym. J.* **2008**, *44*, 3300-3305.
50 C. Dire, J. Belleney, J. Nicolas, D. Bertin, S. Magnet, B. Charleux, *J. Polym. Sci. Part A: Polym. Chem.* **2008**, *46*, 6333-6345.
51 Y. Guillaneuf, D. Gigmes, S. R. A. Marque, P. Astolfi, L. Greci, P. Tordo, D. Bertin, *Macromolecules* **2007**, *40*, 3108-3114.
52 A. C. Greene, R. B. Grubbs, *Macromolecules* **2010**, *43*, 10320-10325.
53 J. Nicolas, C. Dire, L. Mueller, J. Belleney, B. Charleux, S. R. A. Marque, D. Bertin, S. Magnet, L. Couvreur, *Macromolecules* **2006**, *39*, 8274–8282.
54 J. Nicolas, B. Charleux, O. Guerret, S. Magnet, *Macromolecules* **2004**, *37*, 4453-4463.
55 C. Lefay, J. Belleney, B. Charleux, O. Guerret, S. Magnet, *Macromol. Rapid Commun.* **2004**, *25*, 1215-1220.
56 H. M. L. Lambermont Thijs, R. Hoogenboom, C.-A. Fustin, C. Bomal-D'Haese, J.-F. Ghy, U. S. Schubert, *J. Polym. Sci. Part A: Polym. Chem.* **2009**, *47*, 515-522.
57 H. Y. Liu, X. X. Zhu, *Polymer* **1999**, *40*, 6985-6990.
58 R. Xu, *Particle Characterization: Light Scattering Methods*. B. Scarlett (ed.), Kluwer Academic, New York, NY, **2002**.
59 C. Boutris, E. G. Chatzi, C. Kiparissides, *Polymer* **1997**, *38*, 2567-2570.
60 C. Zhang, M. Maric, *Polymers* **2011**, *3*, 1398-1422.
61 J. Y. Huang, K. Matyjaszewski, *Macromolecules* **2005**, *38*, 3577-3583.

711 62 F. J. Hua, X. G. Jiang, D. J. Li, B. Zhao, *J. Polym. Sci. Part A: Polym. Chem.* **2006**, *44*,
712 2454-2467.
713 63 I. Idziak, D. Avoce, D. Lessard, D. Gravel, X. X. Zhu, *Macromolecules* **1999**, *32*, 1260-
714 1263.
715 64 D. Li, W. J. Brittain, *Macromolecules* **1998**, *31*, 3852-3855.
716 65 X. Savelyeva, B. H. Lessard, M. Maric, *Macromol. React. Eng.* **2012**, *6*, 200-212.
717 66 J. E. Chung, M. Yokoyama, T. Aoyagi, Y. Sakurai, T. Okano, *J. Controlled Release*
718 **1998**, *53*, 119–130.